AN ABSTRACT OF THE THESIS OF

Joseph S. Thomas for the degree of Master of Science in Industrial Engineering, presented on August 27 2001. Title: Establishing Thermally-Enhanced Edge Registration (TEER) as a Feasible Alignment Technique for Metallic Microlaminated Devices

Redacted for Privacy

Abstract approved: _____

Brian K. Paul

The paper describes a Thermally-Enhanced Edge Registration (TEER) technique for precision aligning large numbers of laminae in diffusion bonding processes. This technique is particularly relevant for the formation of micro heat exchangers and microreactors requiring highly paralleled microchannel arrays but is also being used to register other laminated devices with precision alignment requirements such as ion traps for quantum computing. The technique uses the difference in thermal expansion between a graphite fixture and metallic laminae to produce a registration force at the bonding temperature. At room temperature, a clearance is designed into the graphite fixture to allow for easy loading of the laminae. At the bonding temperature, the laminae interfere with the side of the fixture producing the registration force. The technique has been extensively studied and found to provide an average layer-to-layer misalignment of 5 microns for laminae with a thickness of 75 microns. The technique provides a plausible means for high-

volume registration of large quantities of laminae when compared with other techniques.

Establishing Thermally-Enhanced Edge Registration (TEER) as a Feasible Alignment Technique for Metallic Microlaminated Devices

By
Joseph S. Thomas

A THESIS
Submitted to
Oregon State University

In partial fulfillment of
the requirements for the
degree of

Master of Science

Presented August 27, 2001
Commencement June 2002

Master of Science thesis of Joseph S. Thomas presented on August 27, 2001

APPROVED

Redacted for Privacy

Major Professor, representing Industrial Engineering

Redacted for Privacy

Department Head of Industrial and Manufacturing Engineering

Redacted for Privacy

Dean of Graduate School

I understand that my thesis will become a part of the permanent collection of Oregon State University libraries. My signature below authorizes release of my thesis to any reader upon request.

Redacted for Privacy

Joseph S. Thomas, Author

TABLE OF CONTENTS

LIST OF FIGURES

LIST OF FIGURES (continued)

LIST OF TABLES

ESTABLISHING THERMALLY-ENHANCED EDGE REGISTRATION (TEER) AS A FEASIBLE ALIGNMENT TECHNIQUE FOR METALLIC MICROLAMINATED DEVICES

INTRODUCTION

Microlamination is the patterning and bonding of thin layers of material, called laminae, to produce a monolithic device with embedded features. The microlamination process involves three steps: laminae patterning, laminae registration and laminae bonding. Figure 1a shows an example of the microlamination of a general-purpose microchannel array, which would be used for micro-scale heat and mass transfer applications.

Microlamination techniques have been used to fabricate microfluidic devices for advanced climate control,[i] solvent separation,[ii] dechlorination,[iii] microcombustion,[iv] fuel processing,[v] high-temperature catalysis,[vi] fluid compression,[vii] microdialysis,[viii] and inkjet print heads[ix] among others. In all, microlamination has been used to construct microtechnology devices in a wide array of materials including copper, stainless steel, intermetallics and various polymers with features as small as tens of micrometers.

In laminated devices, alignment can be an important step in the fabrication of the device. An experiment was carried out to fabricate a microchannel heat exchanger from NiAl.[vi] A micrograph of the device is in Figure 1b. As can be seen, there is a great deal of warpage in the fins of the device. A rudimentary study

was carried out which indicated that buckling contributed to the misalignment (Appendix 5). The effect of this misalignment is flow maldistribution within the heat exchanger creating "hot spots" within the heat exchanger, which is known to greatly reduce its effectiveness.

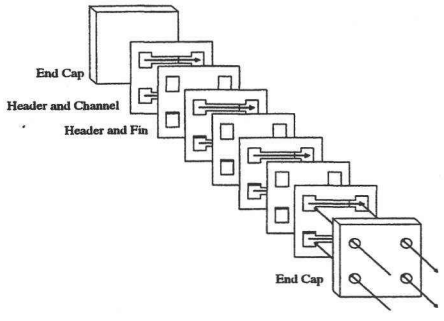

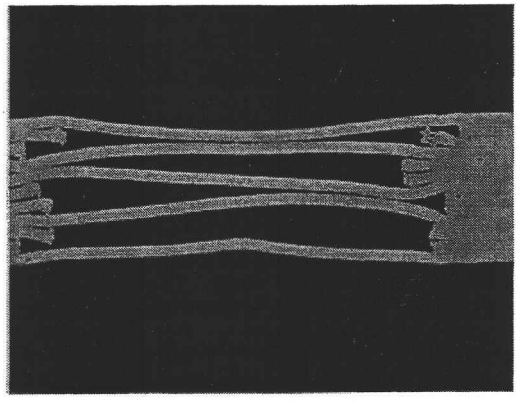

Figure 1a.Microlamination scheme used to fabricate a dual micro-channel array. Arrows show direction of flow. 1b. Micrograph of NiAl microchannel device.

Precision bonding is also important in other applications. Ion traps are used to create, trap and probe highly charged ions. They are made from bonding multiple layers of metal and ceramic with pre-patterned micro-scale features. Radio frequency waves are emitted out from electrodes to produce an electric field. Aligning the electrodes is very important since even a small misalignment can affect the functioning of the ion trap.[x,xi] Estimates of alignment accuracy necessary

for device functioning are on the order of 5 μm. Microvalves as seen in Figure 2 are multi-layered devices that find their use in biological and micro-fluidic systems. The diameter of the chamber is in the 100 μm range, hence aligning of the different layers is crucial for the microvalve to perform well and have high diodicity.[xii] Estimate for alignment accuracy for proper device functioning are well below 20 μm. The MIT micro gas turbine requires precision alignment during wafer bonding of multiple laminae to produce precision air bearings.[xiii] Estimate of alignment accuracy for proper device functioning are below 10 μm. Therefore alignment is important in multi-layered devices and applications.

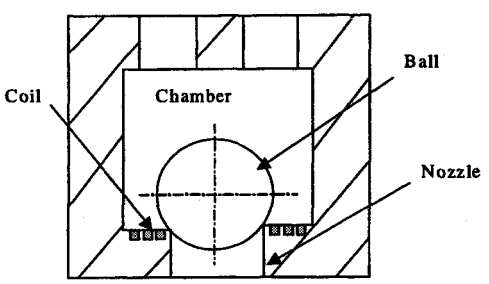

Figure 2. Cross-section of a micro-ball valve

For these and other reasons, precision alignment techniques are needed for bonding in micromanufacturing. Different alignment schemes have been identified and classified into five broad categories namely optical, infrared, self-alignment, pin and edge alignment.

ALIGNMENT SYSTEMS

Optical alignment uses principles of optometry to align substrates and is accomplished in various ways. The mask has transparent windows to align it to the wafer just before x-ray exposure. Alignment to within 5 μm is achieved. [xiv] Through holes are etched in a wafer so that two wafers can be viewed and aligned. If one of the substrates is transparent like glass then it can be aligned to the wafer. Alignment keys are etched on the backside of a wafer and used to align two wafers. A microscope is inserted between two wafers, the wafers are aligned, the microscope is moved away and the wafers are brought together. Two microscopes are placed on the outsides of two wafers and the wafers are aligned. With this technique, alignment to within one μm has been obtained.[xv] Another approach of optical alignment uses in situ interferometers formed from pairs of low-efficiency diffraction microlenses. The resulting interference pattern is projected and used to align two microlenses arrays. Alignment of device planes to within one μm was achieved.[xvi]

Infrared alignment is used in wafer bonding to align wafer segments. One way to align wafers using infrared radiation is to etch grooves into two wafers. Then an infrared image of the two wafers can be projected onto a screen and used for alignment. With this technique alignment to within 5 μm has been achieved. [xvii] Another technique utilizes microstructures (previously exposed patterns that exist on the wafer), which scatters light to either side of the wafer. The alignment

accuracy depends on the wavelength of the light and the angle subtended by the apertures on the wafer. Alignment to within 25nm can be obtained.[xviii]

Another registration technique used for bonding devices is self-alignment. Precision grooves are embossed into metallic substrates to self-align microoptical components like microlenses, optical fibers, glass rods with mirrors. Since etching is used to make grooves is silicon, embossing is used for metals. The component can be laid into the grooves and are aligned. Alignment of about 5 μm is obtained and is good enough for the self-positioning of multimode fibers.[xix]

As suggested, many metallic laminated devices are bonded by solid-state diffusion bonding. In diffusion bonding, the laminae are heated to high temperature and held at a high pressure for a fixed time. At the end of the cycle the laminae form a monolithic device. Optical alignment, infrared alignment and self-alignment are not useful when a high number of laminae need to be aligned during diffusion bonding. Optical techniques are limited to the use of transparent materials. Infrared techniques require the individual repositioning of each lamina relative to the lamina stack, which can be very laborious and time-consuming. In self-alignment, the patterning of laminae can be time consuming and elaborate. This can result in higher cost of fabrication. Traditionally, pin and edge alignment techniques are used to align large numbers of laminae. However, there are some inherent problems with both, pin and edge alignment techniques.

Pin alignment (Figure 3a and 3b) has been used in a variety of precision alignment applications. Grooves are etched in two wafers using planar

photolithography and an alignment pin is placed in one groove. The other wafer is placed over that and rotated until the two grooves coincide. The pin can be removed or left, if it will not interfere with the functioning of the device. Alignment of 5 μm has been achieved.[xx] Pin alignment using press-fit gauge pins was also used to align two level nickel LIGA (X-ray lithography, electrodeposition and molding) structures to within one micron. The pin was first press fit into one substrate and then the other substrate was press fit onto the foundation substrate.[xxi] Pin alignment has also been used to align microchannels in a plastic cross-flow micro flow heat exchanger.[xxii]

There are a few difficulties with pin alignment for high temperature diffusion bonding applications. The locations of the pins have to be very precise with respect to each other. The pins need to be perpendicular to the surface of the fixture. With use, the pins undergo wear and tear. For registering a large number of laminae, pin alignment can be laborious and time consuming. During diffusion bonding, as the fixture and laminae are heated, the fixture, pins and shims can expand at different rates, resulting in warpage of the device. [vi] At the end of the bonding cycle, the pins stick to the device and need to be pulled out. This can result in bending of the device.

Edge alignment is used to align masks to the substrate for multi level optical and x-ray exposures. It uses reference posts to achieve an alignment of 5 μm.[xxiii] An offset mark and a bonding fixture can also be used to align wafers before bonding. This technique matches the patterns on both wafers and aligns them

before they are bonded.[xxiv] Edge alignment (Figure 3c) has the potential to remove the six degrees of freedom to align the laminae, but does require a registration force to constrain the laminae in that position. Slipping of the laminae can be a problem when the device is multi-layered.

Since many metal microlaminated devices are multi-layered and require bonding at a high temperature, none of the techniques mentioned above are suitable for alignment. Proposed is a thermally-enhanced edge registration (TEER) technique for use in high-temperature diffusion bonding of microlaminated devices.

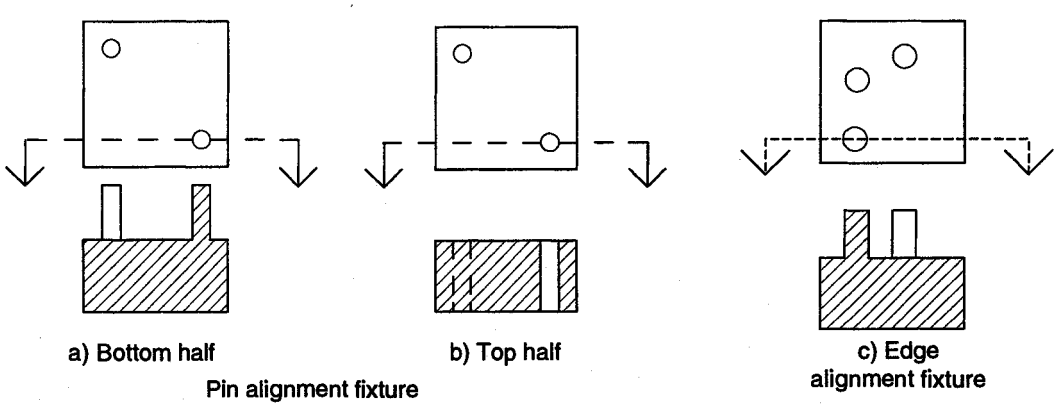

Figure 3. (a) Bottom half of pin alignment fixture (b) Top half of pin alignment fixture (c) Edge alignment fixture

The TEER technique proposed uses the difference in the thermal expansion of the laminae and the fixture to produce a registration force on the laminae at the bonding temperature. The technique involves loading the laminae into a fixture

(Figure 4) made of a material with a smaller coefficient of thermal expansion than the lamina material. At room temperature, a clearance allowance exists between the laminae and the fixture allowing for easy loading of the laminae. At bonding temperature, the laminae interact with the edge of the fixture producing a registration force.

THEORY

The width of the slot in the fixture (Figure 4) is calculated based on the linear thermal expansion of the lamina and the fixture. Let L_1 and L_2 be the device length before and after thermal expansion respectively and let L_3 and L_4 be the width of the slot in the fixture before and after thermal expansion respectively. α_1 is the coefficient of linear thermal expansion of the device material and α_2 is the coefficient of linear thermal expansion of the fixture material. Let dT be the difference in bonding and room temperature.

When the device is heated, the device expands and the new length is given by,

$$L_2 = L_1 + \delta L_1 = L_1(1 + \alpha_1 dT) \qquad (1)$$

The slot in the fixture also expands and the new width is given by,

$$L_4 = L_3 + \delta L_3 = L_3(1 + \alpha_2 dT). \qquad (2)$$

In the TEER technique, the expanded device length and expanded width of the slot should be the same so that the edges of the laminae can interact with the edge of the slot and self-align. Thus, L_2 must equal L_4. Equating (1) and (2), the width of the slot to be machined can be calculated as:

$$L_3 = \frac{L_2}{(1+\alpha_2 dT)} = \frac{L_1(1+\alpha_1 dT)}{1+\alpha_2 dT} \qquad (3)$$

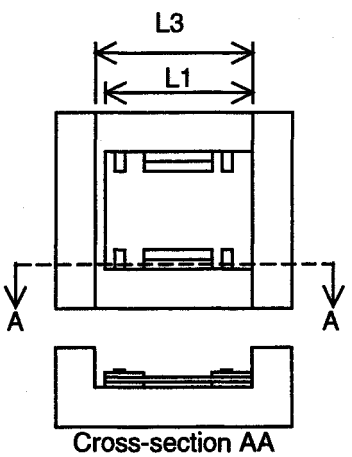

Figure 4. Loading of the laminae into the fixture

EXPERIMENTAL

A registration fixture was designed to align laminae in one direction since it is easier to control alignment in one direction when compared to two directions.

Measurement of misalignment in one direction is also easier. The fixture design for the TEER technique simply involves a through slot in the fixture. For the TEER technique to be successful, the stiffness of the laminae was thought to be crucial. This is because once the laminae are fully expanded, they interfere with the edge of the slot in the fixture. If the laminae are stiff enough, the interference force will realign the laminae. If they are not stiff enough they may deflect or buckle. Since stiffness of the laminae depends on the thickness of the lamina and device length, an experiment was designed in which two factors, thickness of laminae and device lengths were varied. The two factors were varied at two levels and four devices were fabricated at each combination. The two levels of device size were 12.7 mm and 25.4 mm and the thickness of laminae were 50.8 μm and 76.2 μm. An analysis of variance (ANOVA) table was constructed to identify the significant factors in the experiment.

One concern in the process was too much interference at the bonding temperature, which might result in deformation of internal geometries. The laminae in the test article were designed as seen in Figure 5 to readily observe if deformation of internal geometries was an issue. Deformation withing the device was observed by deflection of the fins. The layer-to-layer misalignment was measured through windows in the laminae. This measurement of misalignment was simpler when compared to metallography, which can be laborious and time consuming. There is also a possibility of inducing some warpage in the device during the cutting phase of the metallographic process. Five windows were

patterned on the laminae to have a sense of the orientation of the laminae during registration.

A microlamination process was used to produce the test articles as shown in Figure 5a. The test laminae were patterned from 304 stainless steel shim stock with laser ablation at the 4^{th} harmonic of a Nd:YAG laser (266 nm). Different sized laminae (12.7 and 25.4mm) were patterned at different thicknesses (0.0508 and 0.0762mm). After patterning, the laminae were rinsed with acetone, ethanol and de-ionized water (AED). In an effort to remove the slag and ejecta, the laminae were cleaned in an ultrasonic cleaner with 50% concentration of citranox for 20 minutes and then rinsed again with acetone, ethanol and de-ionized water.

The laminae were stacked in order as seen in Figure 5a. Since the fixture was designed to register the laminae along one direction, adhesive tape was used to initially hold the laminae together in the perpendicular direction as shown in Figure 5b. The laminae were placed in the slot of the fixture such that the edges to be registered were parallel to the slot in the fixture as in Figure 3. The laminae were diffusion bonded in a vacuum hot press. The bonding conditions used were 900^{o} Celsius at 6.55 MPa (950psi) for two hours. During the bonding cycle the vacuum chamber was allowed to heat up to the bonding temperature before the bonding pressure was applied. This was to allow the laminae to register by interference with the edge of the slot in the fixture. During the cooling phase of diffusion bonding the bonding pressure was again removed so that the laminate could contract uniformly without inducing any stress.

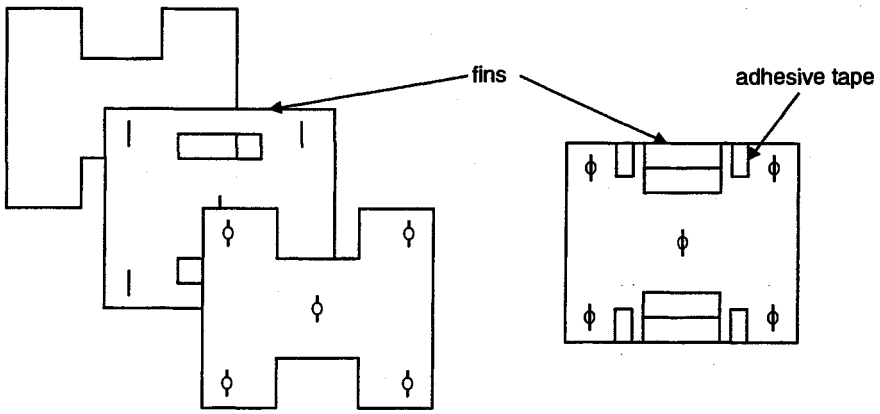

Figure 5. (a) Laminae used to make the test article (b) Laminae initially held together with adhesive tape

The layer-to-layer misalignment was measured using a LEICA DML microscope, which was hooked to a charge-coupled device (CCD) camera and viewed on the screen. A video measuring system was connected to measure the misalignment. The laminae were placed on the stage of the microscope and focused till the registration markers could be seen clearly. The magnification of the microscope was 200X and the resolution, 0.3 – 0.4 μm. One measurement line was aligned with the line marker from the top lamina (the line from both sides of the circular window), the other measurement line was aligned with the line marker from the second lamina (the line in the circular window). The distance between the two lines was the measure of misalignment. This is illustrated in Figure 6. The registration was measured for all 5 windows and recorded. Twenty of the eighty readings were validated with SEM micrographs of which, two examples are shown in Figure 7. A paired t-test was performed and showed no difference in the readings from the SEM and the microscope at a 95% confidence level (Appendix 6).

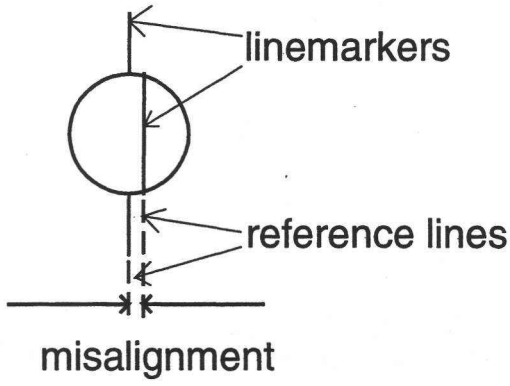

Figure 6. Measuring misalignment at a window with the line markers

Reproducibility of the measurement technique was evaluated by comparing measurement results from three different users. To test for the statistical significance of the user, it was introduced as a factor in an ANOVA. From the ANOVA table, it was concluded at a 95% confidence level that the factor "user" was not significant.

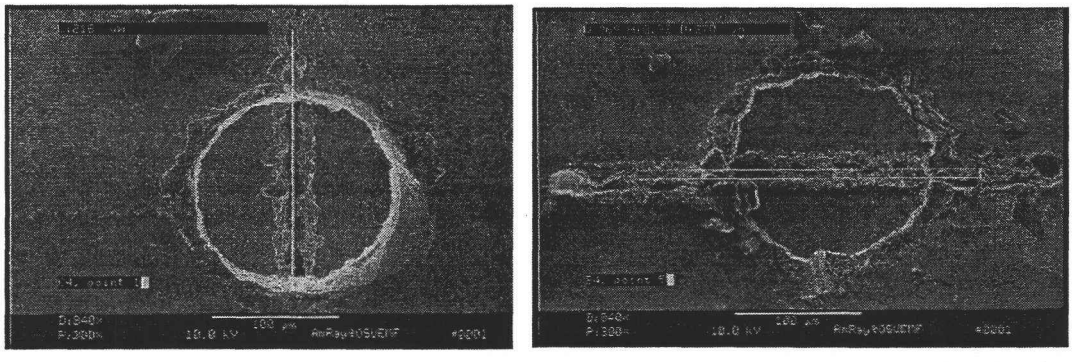

Figure 7. (a) SEM with perfect alignment (b) SEM with misalignment of 8.32 μm

RESULTS AND DISCUSSION

The misalignment was measured on all test devices. An overall average misalignment of 4.3 μm was obtained. The accepted level of misalignment is 50μm.[xxv] The results for each combination are in Table 1.

Thickness of lamina / Device length	50.8 microns	76.2 microns
12.7mm	**3.95μm**	**2.03μm**
25.4mm	**8.09μm**	**3.14μm**

Table 1. Table of misalignment for different device sizes and lamina thickness

The ANOVA table was constructed and it was observed that lamina thickness and device length were significant factors at a 95% confidence level as seen in Figure 8. The misalignment distributions are shown in Figure 8 both as a function of device size and lamina thickness.

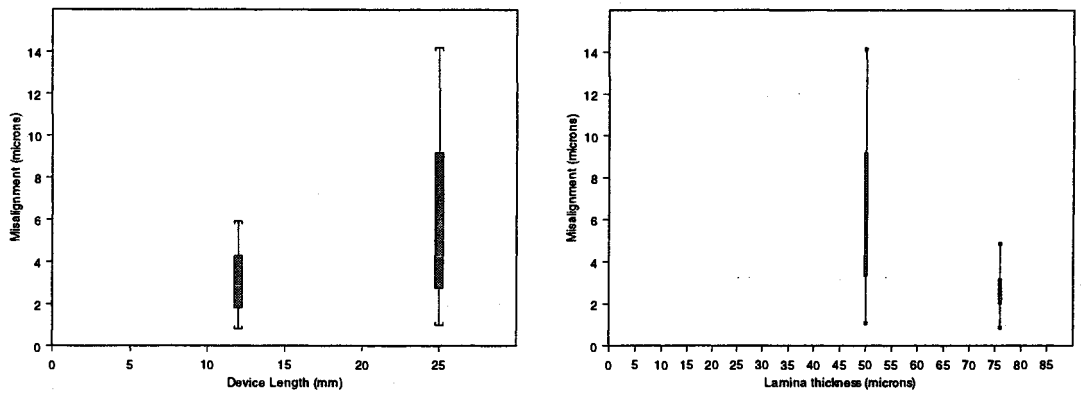

Figure 8. (a) Graph of misalignment versus device length (b) Graph of misalignment versus lamina thickness

The thicker laminae and smaller device size had better alignment and less variability. The smaller device ($\mu = 2.99$, $\sigma = 1.70$) had better alignment and less variability than the larger device ($\mu = 5.61$, $\sigma = 4.09$). Similarly, the thicker laminae ($\mu = 2.59$, $\sigma = 0.96$) had better alignment than the thinner laminae ($\mu = 6.01$, $\sigma = 3.99$) and also had less variability.

To understand why this is so, consider the following. The interference pressure 'P', which is applied on the edge of the laminae during thermal expansion in the diffusion bonding process is given by

$$E = \frac{\sigma}{\varepsilon} = \frac{PL}{A\Delta} \qquad (4)$$

where 'E' is Young's modulus, 'σ' is stress, 'ε' is strain, 'L' is length of the device, 'Δ' is increase in length and 'A' is the cross-sectional area. A is given by

$$A = b * h \tag{5}$$

Where 'b' is the width of the device and 'h' is the thickness of the lamina as seen in Figure 9.

The stiffness of the lamina 'k' is defined as the pressure applied per unit of deformation. Thus,

$$k = \frac{P}{\Delta} \tag{6}$$

Substituting for P and Δ from (4),

$$k = \frac{AE}{L} = \frac{bhE}{L} \tag{7}$$

As seen from the above equation, the stiffness increases with increasing cross-sectional area and decreasing length. This is consistent with the results found in Figure 8. As device dimensions increase in the 'L' dimension, the b/L ratio decreases resulting in a decrease in overall stiffness. Similarly, an increase in the thickness 'h' will result in stiffer laminae and improved registration. It is

interesting to note that stiffness of the laminae would not change if the 'b' and 'L' dimensions changed proportionately. This would suggest that it might be feasible to maintain this level of registration even as the scale of the device was increased.

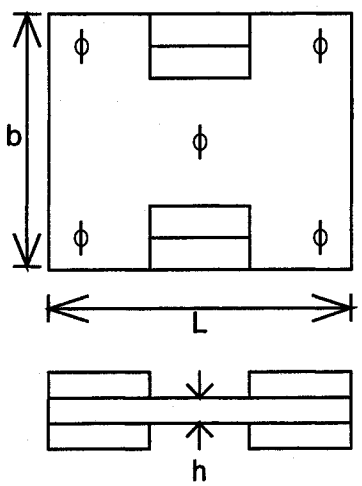

Figure 9. The laminated test device

In the microlamination process there were some sources of variation that could have had an impact on the misalignment. The laser patterning of the lamina is the first step in microlamination. Repeatability of the laser could have been a source of error. The repeatability of the laser has been validated to within two microns. Another source of error could be the ejecta on the front surface of the laminae, which is a by-product of laser ablation. Though the laminae are rinsed and cleaned ultrasonically, some ejecta remains on the laminae. This could hinder

the laminae in registering themselves. The ejecta on the edges could impede the self-aligning process of the laminae during the heating cycle. Hence, the shims remain in their original position and can result in misalignment.

The width of the laser beam (used to pattern the laminae and line markers used in measurement) varied between 20 and 30 μm. The lamina-to-lamina misalignment was measured as the distance between the middle of the line markers on the first and second lamina. Since the line markers are broad, choosing the center of the line markers is subjective and depends on the user.

Finally, some source of error may have been introduced in the tolerances of the graphite fixture. The graphite fixture was machined on a milling machine, which has a resolution of 12.7 μm. The average misalignment obtained using the TEER method was less than 5 μm, which is about 40% the resolution of the milling machine. The implication of this is obvious. Registration below 5 μm is possible with fixtures having tolerances in the tens of microns. This suggests that not only is the process robust, but it also allows for the fixturing with looser tolerances improving the economics of the technique. This can best be explained through Figure 10. Figure 10 is the result of running an experiment where the size of the device was varied relative to the size of the fixture.

Figure 10 clearly shows that the misalignment remains somewhat constant over the interval of interference between the laminae and the fixture. The length of this interval is over 100 μm, which is well in excess of the tolerance of the machine tool. This suggests that the TEER process is able to absorb the tolerance of the

fixture and is therefore robust. It must also be mentioned that the amount of tolerance which may be absorbed decreases with decreasing size of the device. Therefore it is expected that a lower limit exists beneath which the tolerance of the fixture cannot be consistently absorbed and, consequently, the repeatability and robustness of the process begins to suffer.

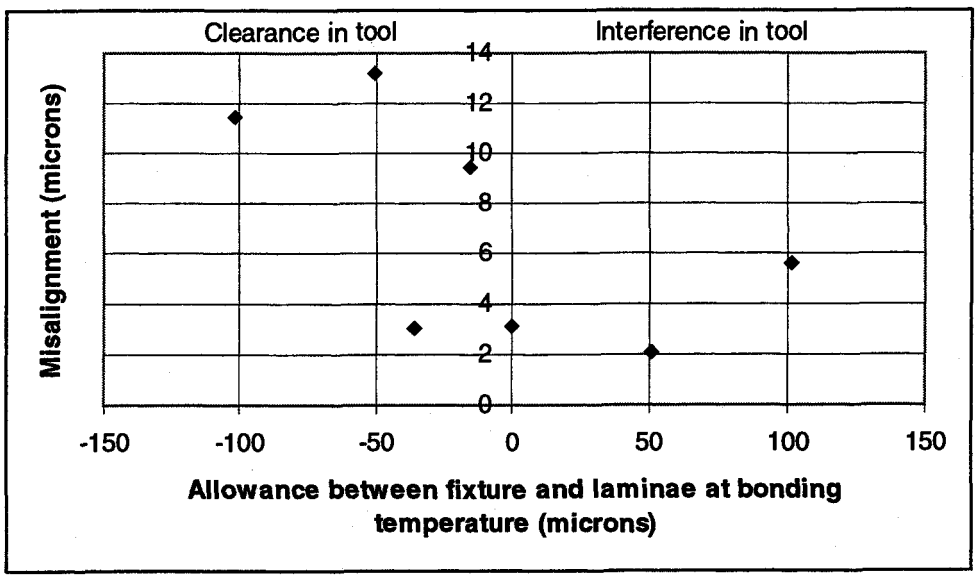

Figure 10. Graph of misalignment versus allowance between fixture and laminae at bonding temperature

Notice also that when a clearance exists between the fixture and the laminae at the bonding temperature, the alignment becomes much more sporadic than when an interference exists. Conversely, it was observed that too large of an interference produces buckling within the fins of the test article. This suggests that a limit may

exist on the allowance of the fixture, which is governed by the desired registration accuracy (in the case of a clearance) and the buckling of the laminae (in the case of inteference)

Other sources of variation in the process would include a static value for the coefficient of thermal expansion for the material of the laminae and fixture (graphite). Further, the temperature sensor in the chamber of the vacuum hot press is located on the edge of the chamber near the heating element. Therefore, the exact temperature of the laminae was not known. To compensate, the laminae were allowed to remain at bonding temperature for approximately one minute before the bonding pressure was applied. This may not have been enough time to permit temperature uniformity for all laminae.

From the results in the alignment between windows, it was noticed that there was variation in the alignment of different windows on the same device. One possible reason for this can be attributed to the misorientation of the device. An ANOVA table for this analysis is shown in Appendix 7. The means for the misalignment for each window is plotted on the schematic of the test article in Figure 11.

Notice that the alignment is best in the lower left corner and gets progressively worse toward the upper right corner. This provides some indication that the device might have consistently rotated around the right corner. To eliminate this problem, future TEER methods could provide constraint along the second axis as well to eliminate additional degrees of freedom. This suggests that

the results obtained in the experiment may be conservative and may be better in practice.

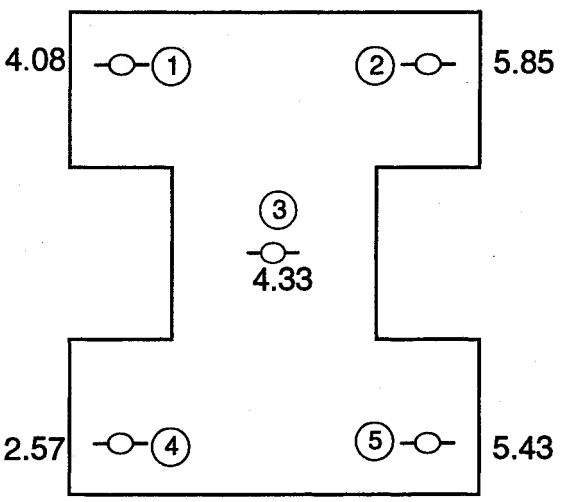

Figure 11. Misalignment at the different windows on the lamina in microns

CONCLUSIONS

A thermally-enhanced edge registration (TEER) technique was introduced for high-temperature diffusion bonding of microlaminated devices with large numbers of laminae. An advantage of this approach is that the fabrication of the fixture is simple and does not require micro-scale precision in order to achieve alignment accuracies below 5 μm. Further, the loading of the fixture is made easy because of the room temperature clearance between the laminae and the fixture. This technique is particularly suitable for highly multi-layered devices that are

diffusion bonded. An average alignment of less than 5 μm was consistently achieved. An average alignment of 2.03 μm was achieved for laminae 75 μm thick and 12.7 mm in length. Thicker laminae were found to register better than thinner laminae. Smaller device sizes also had a positive effect on the registration. From this it can be inferred that the stiffness of the laminae is crucial in the registration of the laminae. It was also shown that there may be optimum allowances between the size of the laminae and the fixture, which are limited by the desired registration accuracy and stiffness of the laminae.

REFERENCES

[i] P. M. Martin, W. D. Bennett, and J. W. Johnson, "Microchannel Heat Exchnagers for Advanced Climate Control," *Proc. SPIE* (v2639, 1996), pp82-88.

[ii] D. W. Matson, P. M. Martin, W. D. Bennett, D. C. Stewart, and J. W. Johnson, "Laser Micromachined Microchaneel Solvent Separator," *Proc. SPIE,* (v3223, 1997), pp253-259.

[iii] G. Jovanovic, J. Zaworski, T. Plant, and B. Paul, *Proc. 3rd Intl. Conf. on Microreaction Technology (Frankfurt, Germany),* 1999, in press.

[iv] D. W. Matson, P. M. Martin, A. Y. Tonkovich and G. L. Roberts, "Fabrication of a Stainless Steel Microchannel Microcombustor Using a Lamination Process," *Proc. SPIE* (v3514, 1998), pp386-392.

[v] A. Y. Tonkovich, J. L. Zilka, Y. Wang, M. J. La Mont, S. Fitzgerald, D. P. Vanderwiel, and R. S. Wegeng, "Microchannel Chemical Reactors for Fuel Processing Applications. II. Compact Fuel Vaporization," *Proc. 3rd Intl. Conf. on Microreaction Technology (Frankfurt, Germany),* 1999, in press

[vi] B. K. Paul, T. Dewey, D. Alman and R.D. Wilson, "Intermetallic Microlamination for High-Temperature Reactors," *4th Int. Conf. Microreaction Tech., Atlanta, GA,* March 5-9, 2000, pp236-243.

[vii] Paul, B.K. and T. Terhaar, "Comparison of two passive microvalve designs for microlamination architectures," *J Micromech. Microengr.,* (v10, 2000), pp15-20.

[viii] P. M. Martin, D. W. Matson, W. D. Bennett, and D. J. Hammerstrom, "Fabrication of plastic microfluidic components," *Proc. SPIE* (v3515, 1998), pp172-176.

[ix] J.J. Anderson, U.S. Patent 4,875,619, Brazing of Ink Jet Print Head Components Using Thin Layers of Braze Material

[x] Q. A. Turchette, D. Kielpinski, B. E. King, D. Leibfried, D. M. Meekhof, C. J. Myatt, M. A. Rowe, C. A. Sackett, C. S. Wood, W. M. Itano, C, Monroe, and D. J. Wineland, "Heating of trapped ions from the quantum ground state", www.lanl.gov, 2000, in press

[xi] Sackett, Klelpinski, King, Langer, Meyer, Myatt, Rowe, Turchette, Itano, Wineland, Monroe, "Experimental entanglement of four particles", Nature, vol 404, pages 256-258, March 2000

[xii] W. Wangwatcharakul and B. K. Paul, "Development of Passive Micro-ball valve" 2001, in press.

[xiii] S. Ashley, "Turbines on a dime", Mechanical engineering magazine online, October 1997

[xiv] C. Khan-Malek, R. Wood, Z. Ling, B. Dudley and S. Stadler, "Multi-Level exposures and 3-D X-ray patterning for high aspect ratio microstructures", Microelectronic Engineering, 41/42, pages 493-496,1998.

[xv] A.R. Mirza, "One Micron Precision, Wafer-Level Aligned Bonding for Interconnect, MEMS and Packaging Applications", Electronics Components and Technology Conference, pages 676-680, 2000.

[xvi] B. Robertson, Y. Liu, G. C. Boisset, M. R. Tagizadeh and D V. Plant, 'In situ interferometric alignment systems for the assembly of microchannel relay systems', Applies Optics, Vol 36, No 35, pages 9253-9260, December, 1997.

[xvii] R.W Bower, M. S. Ismail and S.N. Farrens, "Aligned Wafer Boding: A key to three Dimensional Microstrucures", Journal of Electronic Materials, Vol. 20, No.5, pages 383-387, 1991.

[xviii] G. Wyntjes, M. Hercher, "Wafer alignment based on existing structures", Integrated Circuit Metrology, Inspection and Process Control V, SPIE Vol. 1464, pages 539-545, 1991.

[xix] M. Rode and B. Hillerich, "Self-Aligned positioning of microoptical components by precision prismatic grooves impressed in metal" IEEE Journal of Microelectromechanical systems, Vol 8, No.1, pages 58-64, March, 1999

[xx] R. L. Smith and S. D. Collins, "A wafer-to-wafer Alignment Technique", Sensors and Actuators, 20, 1989, pg 315-316.

[xxi] T. R. Christenson, D. T. Schmale, "A batch wafer scale LIGA assembly and packaging technique via diffusion bonding", MEMS, Twelfth IEEE International Conference on Micro-Electro Mechanical Systems, Technical digest, pages476-481, Orlando Florida USA January 17-21 1999,

[xxii] C. Harris, M. Despa and K. Kelly, "Design and Fabrication of a Cross Flow Micro Heat Exchanger", Journal of Microelectromechanical Systems, vol 9, No 4, pages 502-508, December, 2000

[xxiii] Z. Ling, K Lian and J Goettert, "Passive alignment and its applications in multi-level x-ray lithography", Materials and Device Characterization in micromachinin III, Proceedings of SPIE vol.4175 (2000) 18-19 September 2000, Santa Clara. USA

[xxiv] Y Chou, "Angular alignment for wafer bonding", SPIE, vol.2879 pages 291-297

[xxv] Madou M, 'Fundamentals of Microfabrication', 1997

BIBLIOGRAPHY

Anderson J. J., U.S. Patent 4,875,619, Brazing of Ink Jet Print Head Components Using Thin Layers of Braze Material

Ashley S., "Turbines on a dime", Mechanical engineering magazine online, October 1997

Bower R. W., M. S. Ismail and S.N. Farrens, "Aligned Wafer Boding: A key to three Dimensional Microstrucures", Journal of Electronic Materials, Vol. 20, No.5, pages 383-387, 1991

Chou Y., "Angular alignment for wafer bonding", SPIE, vol.2879 pages 291-297

Christenson T. R., D. T. Schmale, "A batch wafer scale LIGA assembly and packaging technique via diffusion bonding", MEMS, Twelfth IEEE International Conference on Micro-Electro Mechanical Systems, Technical digest, pages476-481, Orlando Florida USA January 17-21 1999,

Harris C., M. Despa and K. Kelly, "Design and Fabrication of a Cross Flow Micro Heat Exchanger", Journal of Microelectromechanical Systems, vol 9, No 4, pages 502-508, December, 2000

Jovanovic G., J. Zaworski, T. Plant, and B. Paul, *Proc. 3rd Intl. Conf. on Microreaction Technology (Frankfurt, Germany),* 1999, in press

Khan-Malek C., R. Wood, Z. Ling, B. Dudley and S. Stadler, "Multi-Level exposures and 3-D X-ray patterning for high aspect ratio microstructures", Microelectronic Engineering, 41/42, pages 493-496,1998.

Ling Z., K Lian and J Goettert, "Passive alignment and its applications in multi-level x-ray lithography", Materials and Device Characterization in micromachinin III, Proceedings of SPIE vol.4175 (2000) 18-19 September 2000, Santa Clara. USA

Madou M, 'Fundamentals of Microfabrication', 1997

Martin P. M., W. D. Bennett, and J. W. Johnson, "Microchannel Heat Exchnagers for Advanced Climate Control," *Proc. SPIE* (v2639, 1996), pp82-88.

Martin P. M., D. W. Matson, W. D. Bennett, and D. J. Hammerstrom, "Fabrication of plastic microfluidic components," *Proc. SPIE* (v3515, 1998), pp172-176.

Matson D. W., P. M. Martin, W. D. Bennett, D. C. Stewart, and J. W. Johnson, "Laser Micromachined Microchaneel Solvent Separator," *Proc. SPIE,* (v3223, 1997), pp253-259.

Matson D.W., P. M. Martin, A. Y. Tonkovich and G. L. Roberts, "Fabrication of a Stainless Steel Microchannel Microcombustor Using a Lamination Process," *Proc. SPIE* (v3514, 1998), pp386-392.

Mirza A.R., "One Micron Precision, Wafer-Level Aligned Bonding for Interconnect, MEMS and Packaging Applications", Electronics Components and Technology Conference, pages 676-680, 2000.

Paul B. K., T. Dewey, D. Alman and R.D. Wilson, "Intermetallic Microlamination for High-Temperature Reactors," *4th Int. Conf. Microreaction Tech., Atlanta, GA,* March 5-9, 2000, pp236-243.

Paul, B.K. and T. Terhaar, "Comparison of two passive microvalve designs for microlamination architectures," *J Micromech. Microengr.,* (v10, 2000), pp15-20.

Robertson B., Y. Liu, G. C. Boisset, M. R. Tagizadeh and D V. Plant, 'In situ interferometric alignment systems for the assembly of microchannel relay systems', Applies Optics, Vol 36, No 35, pages 9253-9260, December, 1997.

Rode M. and B. Hillerich, "Self-Aligned positioning of microoptical components by precision prismatic grooves impressed in metal" IEEE Journal of Microelectromechanical systems, Vol 8, No.1, pages 58-64, March, 1999

Sackett, Klelpinski, King, Langer, Meyer, Myatt, Rowe, Turchette, Itano, Wineland, Monroe, "Experimental entanglement of four particles", Nature, vol 404, pages 256-258, March 2000

Smith R. L. and S. D. Collins, "A wafer-to-wafer Alignment Technique", Sensors and Actuators, 20, 1989, pg 315-316.

Tonkovich Y., J. L. Zilka, Y. Wang, M. J. La Mont, S. Fitzgerald, D. P. Vanderwiel, and R. S. Wegeng, "Microchannel Chemical Reactors for Fuel Processing Applications. II. Compact Fuel Vaporization," *Proc. 3rd Intl. Conf. on Microreaction Technology (Frankfurt, Germany),* 1999, in press

Turchette Q. A., D. Kielpinski, B. E. King, D. Leibfried, D. M. Meekhof, C. J. Myatt, M. A. Rowe, C. A. Sackett, C. S. Wood, W. M. Itano, C, Monroe, and D. J. Wineland, "Heating of trapped ions from the quantum ground state", www.lanl.gov, 2000, in press

Wangwatcharakul W. and B. K. Paul, "Development of Passive Micro-ball valve" 2001, in press.

Wyntjes G., M. Hercher, "Wafer alignment based on existing structures", Integrated Circuit Metrology, Inspection and Process Control V, SPIE Vol. 1464, pages 539-545, 1991.

APPENDICES

APPENDIX A. DESIGN AND DATA FROM EXPLORATORY RUNS

For the exploratory runs, ten samples were microlaminated. The size of the devices was 25.4 mm and had a thickness of 76.2 μm. The bonding conditions used were 6.55 MPa at 900°C for two hours.

The design of the devices are in Figure 12.

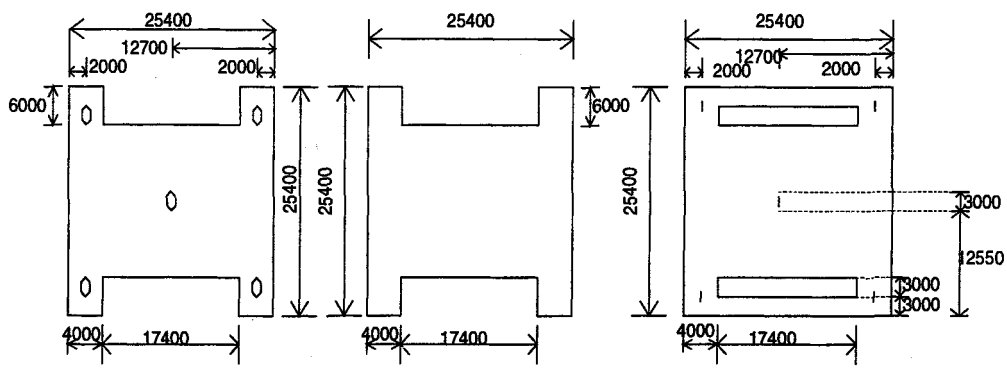

Figure 12. Design of the laminae in the test article.

The first two devices had a window as shown in Figure 13 (a). The third to tenth laminae had windows as shown in Figure 13 (b).

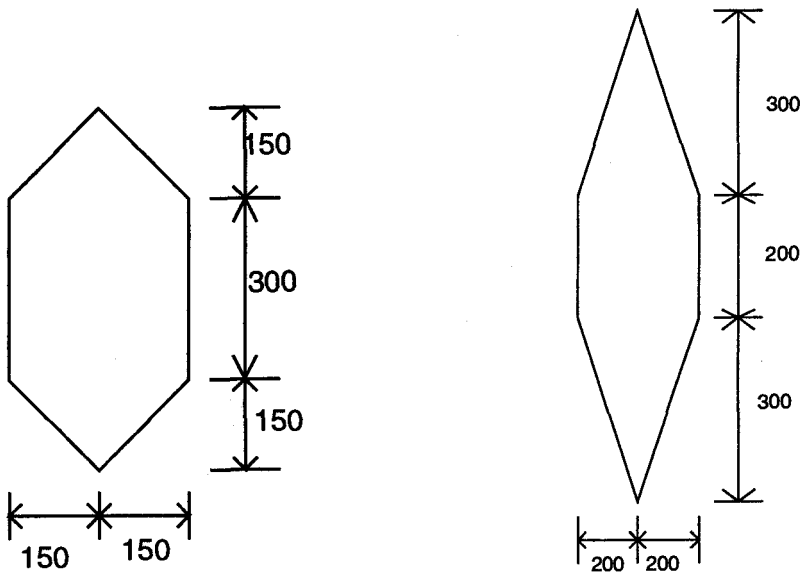

Figure 13 (a) window in the first two devices (b) windows on the third to tenth devices

The misalignment readings from the ten devices were tabulated and can be seen in Table 2.

Sample No	window 1	window 2	window 3	window 4	window 5	Total	Mean
1	5	2	0	2	0	9	1.8
2	0	5	12	2	4	23	4.6
3	2	0	8	8	7	25	5
4	0	1	8	2	0	11	2.2
5	20	0	9	2	0	31	6.2
6	6	2	0	3	5	16	3.2
7	6	6	6	11	0	29	5.8
8	7	11	17	0	4	39	7.8
9	5	6	3	5	3	22	4.4
10	9	10	6	13	9	47	9.4
Total	60	43	69	48	32	252	5.04

Table 2. Misalignment readings from the ten exploratory devices

APPENDIX B. DESIGN OF EXPERIMENT

An experiment was designed based on the results from the exploratory runs. The factors chose for this experiment were lamina thickness and device. It was thought that these two factors affected registration and their significance was tested. They were both varied at two levels as shown below in Table 3.

Factor	12.7 mm	25.4 mm
50.8 μm		
76.2 μm		

Table 3. Table with the factors used in the experiment and their levels

A null and alternated hypothesis was proposed.

Null Hypothesis – There is no significant difference in the misalignment with the varying of the factors.

Alternate Hypothesis – There is a significant difference in the misalignment with the varying of the factors.

The sample size was then calculated for the experiment, so that the results would be statistically significant. Sample size was calculated from operating characteristic curves based on the formula $\phi^2 = \frac{naD^2}{2b\sigma^2}$ (8)

Where

'a' = number of levels for factor A = 2

'b' = number of levels for factor B = 2

'D' = the minimum difference of any two rows or columns = 5 microns

'σ^2' = variance of the samples

'n' = number of samples

'α' = Probability of type I error which is the probability of rejecting the null hypothesis when it is actually true = 0.05

β = Probability of type II error which is the probability of accepting the null hypothesis when it is false

1-β= power of the experiment

'v_1' = numerator degrees of freedom = a-1

'v_2' = error degrees of freedom = ab(n-1)

The variance was obtained from the results from the exploratory runs.

Substituting the values in the equation, we get.

$$\phi^2 = \frac{naD^2}{2b\sigma^2} = \frac{n*2*5^2}{2*2*5.67} = 2.20n \qquad (9)$$

The readings were tabulated for different values of 'n' which is number of samples till the probability of type II error is acceptable. This is tabulated in Table 4.

N	ϕ^2	ϕ	V_1	V_2	β
2	4.4	2.09	1	4	0.
3	6.6	2.56	1	8	0.15
4	**8.8**	**2.96**	**1**	**12**	**0.03**
5	11	3.31	1	16	0.015

Table 4.Table of Type II error with sample size

As seen, four samples are sufficient for an acceptable value of Type II error.

APPENDIX C. EXPERIMENTAL PROCEDURE FOR PATTERNING, ALIGNING, BONDING AND MEASUREMENT OF MICROLAMINATED DEVICES

1. Procedure for patterning

a. Cut the specimen with scissors to about ½" inch larger than the intended patterned size.

b. Create the pattern file in SmartCAM and export it to the laser.

c. Place the shims on the shoulders on the stage of the laser and hold it down with adhesive tape.

d. Focus the laser on the surface of the shim till it can be seen clearly on the video screen.

e. Set the tool path parameters of the laser to the following conditions.

- Profile speed = 4.5 mm/seconds
- Repetition rate = 4500 Hz
- Bite size = 1.0 micron

Set the laser to the external trigger mode with direct current 20.5 A and frequency 4.5 kHz. With these conditions the power is 200mwatts. Increase the current if needed to maintain the power of the laser

f. Check the power of the laser before and after cutting and make sure that it is constant.

g. Set the laser to the internal mode to check the power of the laser with a power meter.

h. Run the program till the laser cuts through the shim. For 0.0762 mm stainless steel, 15 repetitions are used as seen in Figure 12 (a).[1]

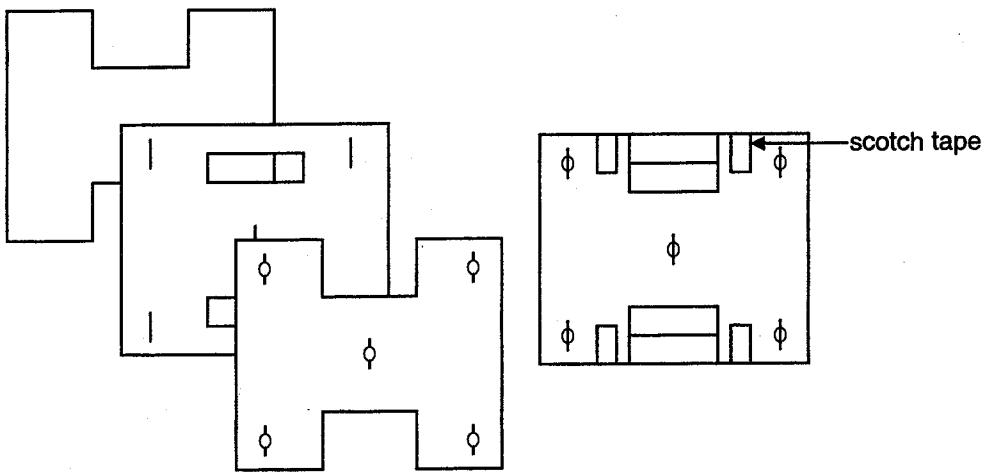

Figure 14. (a) Laminae used to make test article (b) Laminae initially held together with adhesive tape

2. Procedure for bonding

a. Wash the patterned shims with acetone, ethanol and distilled water (AED wash) and blow dry with air.

b. Place the shims in the ultrasonic cleaner with 50% concentrate Citranox for about 20 minutes to remove the slag and ejecta created from laser machining.

[1] For more details refer the safety and operation manual.

c. Wash the shims with acetone, ethanol and distilled water and blow dry with pressurized air.

d. Clean the graphite fixture and apply a thin layer of magnesium hydroxide on the fixture. Dry the magnesium hydroxide in air.

e. Stack the shims in the prearranged order and hold them together with scotch tape in the direction in which the alignment is not critical as shown in Figure 14 (b).

f. Place the fixture centered on the ram of the hot press as shown in Figure 15.

g. Close the chamber and screw on the three knurled nuts.

h. Program the hot press for the bonding cycle, with a heating rate of 30°C/min to 900°C for two hours.

i. Turn the mechanical pump on to lower the air pressure in the chamber.

j. When the pressure reaches 200 milliTorr turn the vacuum pump and the chiller on.

k. Once the required pressure has been reached, start the bonding cycle. The chamber is heated to 900°C at a rate 30°C/minute.

l. When the temperature reaches 900°C bring the rams together and apply a pressure of 6.55MPa (the reading on the dial is the force, hence the area of the specimens is multiplied by the required pressure to get the necessary force).

m. At the end of the two hours retract the two rams so that there is no pressure on the fixture.

n. Allow the hot press to cool down to room temperature.

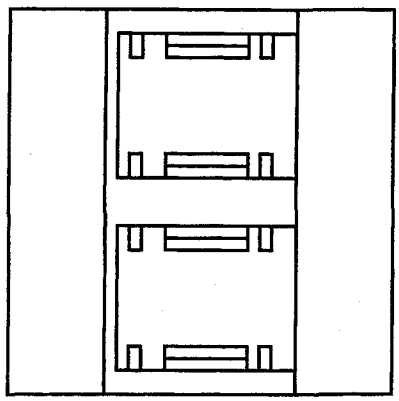

Figure 15. Stack of laminae placed in the alignment fixture

o. Wash the devices with AED solution and blow-dry them in air.

p. Place the devices in the ultrasonic cleaner for about 20 minutes to remove the ejecta.

q. Wash the devices with AED wash and blow dry them in air.

3. **Procedure for measurement of alignment**

In order to measure the misalignment of the edge alignment technique, the diamond window and a line marker are created on the top and second stainless steel laminae. Upon alignment and bonding, all 5 line markers should be located at the center of the diamond window when looking from the top view. Whenever the

laminae are not perfectly aligned to each other, misalignment can happen. For edge alignment, only one direction is concerned for this measurement. In this case, the misalignment of edge alignment technique can be evaluated by measuring the distance between the line marker and the connect line of the diamond window or referred as a reference line as seen in Figure 16.

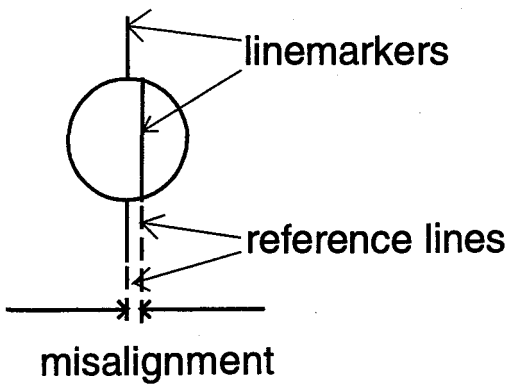

Figure 16. Sketch to illustrate the method of measurement of misalignment

The following section explains the misalignment measurement of the edge alignment technique by implementing the video measurement system[2] and an optical microscope.

a. Turn on the optical microscope and the video measurement system.
b. Make sure that the pointer on the monitor screen is located beside the XY mode and MEASURE command, then press SELECT to enter the XY measurement mode[3].

[2] The video measurement systems must be calibrated prior to this measurement. Consult page 28-39 in the VIA-100 manual for the system calibration.
[3] Consult page 45-47 in the VIA manual for more detail in XY measurement

c. Put the specimen on the microscope stage.

d. Use the 20X objective lens to measure the misalignment with 200X magnification[4].

e. Focus the feature of interest; make sure the video screen cover an entire diamond window. (Note: the line marker should lie on X direction or horizontal axis: as shown on the figure)

f. Set the scale factor of the VIA system to 200X measurement[5], otherwise the user must change the measurement scale to this scale factor[6].

g. On the VIA controller, place the AXIS switch in the Y position and set the COMPARE switch to the OFF position.

h. With the left knob on the controller, position a measurement line to cross through the left corner of the diamond window and the other corner on the right side; this line will be referred as the reference line.

i. With the right knob on the controller, position another measurement line at the centerline of the line marker.

j. The number showing on the screen (for Y value) will be the value of misalignment, which is the distance between the reference line and the center of the line marker.

To verify that the number that we get from this measurement technique is correct, the SEM image is required. As mentioned previously, the resolution of the VIA system for 200X magnification is around 0.5 micron. With the SEM, the

[4] With 200X magnification, the resolution of the measurement is about 0.3-0.5 micron.
[5] The top right corner of the screen should show SF3 = 0200
[6] Consult page 38-39 in the VIA manual for changing the scale factor

resolution of the measurement can be under 0.1 micron dependent on the degree of magnification. Moreover, with the advantage in high depth of field, the image from the SEM will be more precise than from the optical microscope. Therefore, the SEM will be applied to validate the results from this VIA measurement.

APPENDIX D. READINGS FROM THE EXPERIMENT

The main experiment was carried out and three different users noted the readings. This was done to establish the reproducibility of the measurement technique being used. The readings from the three users are in Table 5 below.

User 1

Lamina	Dev size	Code	Window 1	Window 2	Window 3	Window 4	Window 5	Total	Average
2mil	0.5"	A1	5.4	1.5	1	2	8.8	18.7	3.74
2mil	0.5"	A2	3.9	10.3	9.3	1.5	0	25	5
2mil	0.5"	A3	0	2.9	0	4.4	0	7.3	1.46
2mil	0.5"	A4	7.8	1	0	1	18.1	27.9	5.58
2mil	1.0"	B1	3.4	14.2	8.3	2	10.8	38.7	7.74
2mil	1.0"	B2	6.9	0	0	0	1	7.9	1.58
2mil	1.0"	B3	2	14.2	16.7	7.8	12.7	53.4	10.68
2mil	1.0"	B4	15.2	19.1	18.6	3.9	5	61.8	12.36
3mil	0.5"	C1	2	1	2.9	0.5	4.4	10.8	2.16
3mil	0.5"	C2	1	0.5	1	0.5	1	4	0.8
3mil	0.5"	C3	1	0.5	2	4.4	1.5	9.4	1.88
3mil	0.5"	C4	2.9	2.9	4.4	2.9	3.4	16.5	3.3
3mil	1.0"	D1	0	1.5	2.9	2.9	6.9	14.2	2.84
3mil	1.0"	D2	2.9	1	2.5	6.9	0	13.3	2.66
3mil	1.0"	D3	1	4.9	7.8	0	5.9	19.6	3.92
3mil	1.0"	D4	2	5.9	2.5	1	4.4	15.8	3.16
									68.86
									4.30375

Table 5 (a) Readings from User 1 in microns

User 2

Lamina	Dev size	Code	Window 1	Window 2	Window 3	Window 4	Window 5	Total	Average
2mil	0.5"	A1	5	3	1.5	1.5	7	18	3.6
2mil	0.5"	A2	6	10	7.5	6	0	29.5	5.9
2mil	0.5"	A3	1	2.5	2	4	0	9.5	1.9
2mil	0.5"	A4	4	0	1	1	19	25	5
2mil	1.0"	B1	3	13	3	5	10	34	6.8
2mil	1.0"	B2	6	1	0	4	4	15	3
2mil	1.0"	B3	7	19	20	8	17	71	14.2
2mil	1.0"	B4	13	20	18	7	5	63	12.6
3mil	0.5"	C1	2	4	0.5	1	3	10.5	2.1
3mil	0.5"	C2	5	4	2	2	0.5	13.5	2.7
3mil	0.5"	C3	4	6	1	2	2.5	15.5	3.1
3mil	0.5"	C4	2	6	2	1	4	15	3
3mil	1.0"	D1	1	3	3	0	4	11	2.2
3mil	1.0"	D2	0	2	1	4	0	7	1.4
3mil	1.0"	D3	3	7	5	0	8	23	4.6
3mil	1.0"	D4	5	4	3	1	3	16	3.2
									75.3
									4.70625

Table 5 (b)

Lamina	Dev size	Code	Window 1	Window 2	Window 3	Window 4	Window 5	Total	Average
2mil	0.5"	A1	4.4	4.9	2	5.4	7.4	24.1	4.82
2mil	0.5"	A2	8.3	11.3	5.9	1	0.5	27	5.4
2mil	0.5"	A3	0	2.5	1	2.9	0.5	6.9	1.38
2mil	0.5"	A4	2.5	0.5	0.05	1	1	5.05	1.01
2mil	1.0"	B1	4.4	13.2	10.3	0.5	20.6	49	9.8
2mil	1.0"	B2	9.3	3.9	1	2	13.7	29.9	5.98
2mil	1.0"	B3	4.9	14.2	12.7	7.8	3.4	43	8.6
2mil	1.0"	B4	13.2	16.2	13.2	4.9	17	64.5	12.9
3mil	0.5"	C1	1.5	2.9	2.5	2	2.9	11.8	2.36
3mil	0.5"	C2	3.4	0.5	0.5	0	2.5	6.9	1.38
3mil	0.5"	C3	2.5	2	0.5	1.5	2	8.5	1.7
3mil	0.5"	C4	3.9	7.8	2	0.5	2.9	17.1	3.42
3mil	1.0"	D1	1	0.5	2.5	0.5	6.4	10.9	2.18
3mil	1.0"	D2	0.5	1.5	0	2	1	5	1
3mil	1.0"	D3	6.4	7.4	0.5	2.5	7.8	24.6	4.92
3mil	1.0"	D4	5.4	5.9	2.9	0	0.5	14.7	2.94
									69.79
									4.361875

Table 5 (c)

The readings from the tables were used to construct the ANOVA table (Table 6). As can be seen from the table, Device size, lamina thickness and windows are significant factors. User is not significant. This tells us that the measurement technique is repeatable and reproducible.

Analysis of Variance for Misalignment - Type III Sums of Squares

Source	Sum of Squares	Df	Mean Square	F-Ratio	P-Value
MAIN EFFECTS					
A:Thickness	808.685	1	808.685	51.02	0.0000
B:Size	489.776	1	489.776	30.90	0.0000
C:Window	317.21	4	79.3026	5.00	0.0007
D:User	7.57277	2	3.78639	0.24	0.7877
INTERACTIONS					
AB	307.474	1	307.474	19.40	0.0000
AC	63.5238	4	15.8809	1.00	0.4075
AD	1.86119	2	0.930594	0.06	0.9430
BC	114.405	4	28.6012	1.80	0.1292
BD	7.49102	2	3.74551	0.24	0.7897
CD	38.1194	8	4.76493	0.30	0.9651
RESIDUAL	3328.43	210	15.8497		
TOTAL (CORRECTED)	5484.54	239			

All F-ratios are based on the residual mean square error.

Table 6. ANOVA table

A Post-Hoc comparison was carried out between the different levels in each factor.

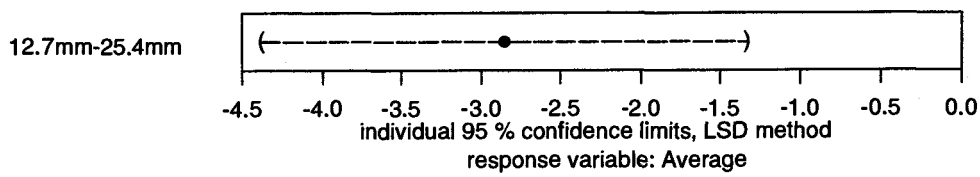

Figure 17 (a) Comparison of different levels in the factor device size.

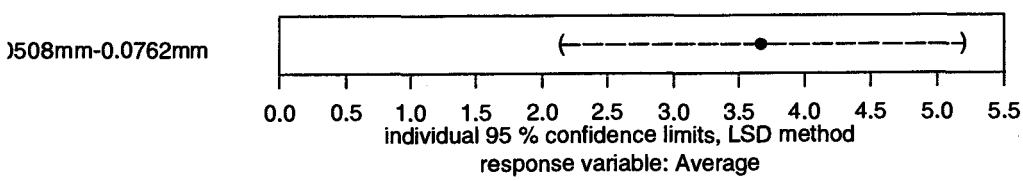

Figure 17 (b) Comparison of different levels in the factor lamina thickness

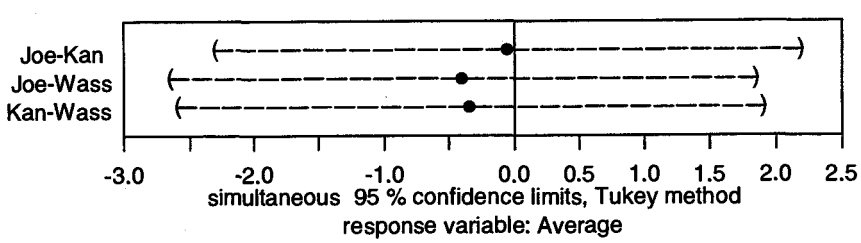

Figure 17 (c) Comparison of readings from the different users

APPENDIX E. EFFECT OF MISALIGNMENT ON WARPAGE

The effect of misalignment of microchannels was modeled in a fluidic system. A multi-layer microfluidic system consists of alternating layers of microchannels, which allows the fluids to flow in two directions separated by fins. The schematic is shown in the Figure 18.

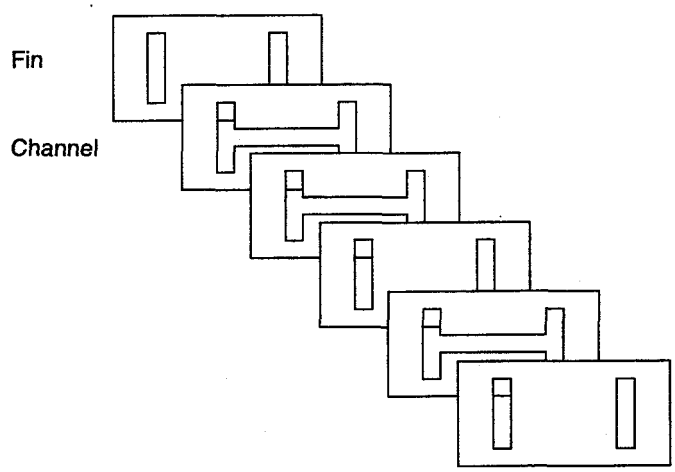

Figure 18. Schematic of microfluidic array

Once the laminae are registered and bonded the plan view of the stack is as in Figure 19. This is assuming that there is perfect registration in the laminae.

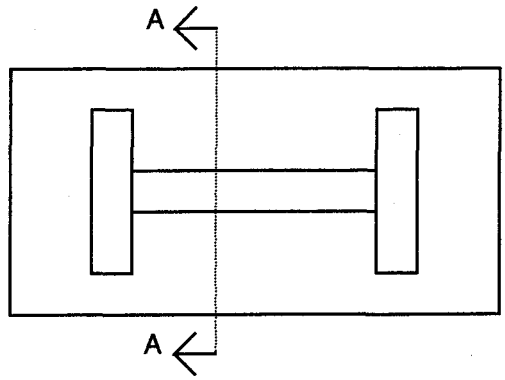

Figure 19. Plan view of the stack of laminae

In the bonding the multi-layer devices, equal bonding pressure is applied to both sides of the laminae. If there is misalignment between two layers, such as point A and B as in Figure 20, there is part of the channel that is not supported on the other side of the fin. This induces a bending moment and can deflect the fin.

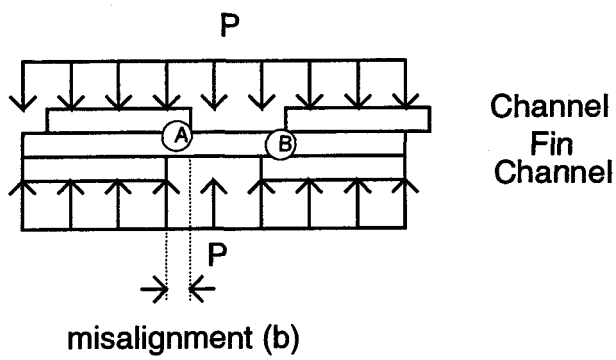

Figure 20. Cross-sectional view at section AA

A free body diagram of the fin was developed and is shown in Figure 21. Let the beam have length 'L', misalignment 'b' and width 'd'. A bonding pressure of 'p' is applied over the whole surface of the device. 'w' is the force per unit length along the length of the beam and is given by $w = pd$

It is assumed that the two ends of the fin are fixed. Due to this there is a vertical load V_A and V_B and bending moments M_A and M_B acting at the ends of the beam.

Equation for bending moment in a beam is given by

$$EI\frac{d^2y}{dx^2} = M_{XX} \qquad (10)$$

Consider the section XX, at a distance of x from the left end of the beam. The bending moment about that point is given by

$$M_{XX} = V_A x - M_A - bw(x - b/2) \qquad (11)$$

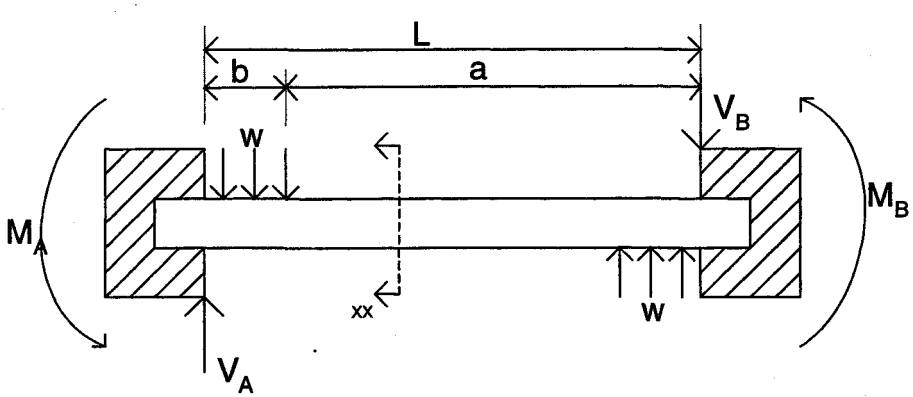

Figure 21. Free body diagram of the beam

Substitute for M_{XX} from equation (11)

$$EI\frac{d^2y}{dx^2} = V_A x - M_A - bwx + \frac{b^2 w}{2} \qquad (12)$$

Integrate equation (12) twice to get,

$$EI\frac{dy}{dx} = \frac{V_A x^2}{2} - M_A x - \frac{bwx^2}{2} + \frac{b^2 wx}{2} \qquad (13) \text{ and}$$

$$EIy = \frac{V_A x^3}{6} - \frac{M_A x^2}{2} - \frac{bwx^3}{6} + \frac{b^2 wx^2}{4} \qquad (14)$$

For beams with fixed ends the following boundary conditions are applied

$$(1)\ x = L, \frac{dy}{dx} = 0 \qquad (15)$$

$$(2)\ x = L,\ y = 0 \qquad (16)$$

Substituting (15) and (16) in (13) and (14) and solving, we get

$$V_A = bw \quad \text{and} \qquad (17)$$

$$M_A = \frac{b^2 w}{2} \qquad (18)$$

Maximum moment on the beam is given by,

$$M_A = \frac{b^2 w}{2} \qquad (19)$$

From the bending equation, the maximum elastic moment is given by

$$M_E = \frac{dh^2 \sigma_y}{6} \qquad (20)$$

Now equating equations (19) and (20) and substituting $w = pd$, we get

$$b^2 = \frac{h^2 \sigma_y}{3p} \qquad (21)$$

Hence the maximum allowable, b, misalignment depends on the yield stress of the material, the thickness of the material and the bonding pressure that is applied.

APPENDIX F. REPRODUCIBILITY OF THE MEASUREMENT TECHNIQUE

The misalignment was measured on four devices to validate the reproducibility of the measurement technique. They are tabulated in Table 7.

Code	User	Window 1	Window 2	Window 3	Window 4	Window 5	Total	Average
A1	SEM	4.48	3.2	5.12	8.32	7.68	28.8	5.76
B3	SEM	7.68	21.1	25.6	6.4	15.4	76.18	15.236
B4	SEM	11.5	19.2	16.3	0	8.32	55.32	11.064
C4	SEM	0	3.2	3.84	7.04	5.65	19.73	3.946
A1	JOE	5.4	1.5	1	2	8.8	18.7	3.74
B3	JOE	2	14.2	16.7	7.8	12.7	53.4	10.68
B4	JOE	15.2	19.1	18.6	3.9	5	61.8	12.36
C4	JOE	2.9	2.9	4.4	2.9	3.4	16.5	3.3
A1	WASS	5	3	1.5	1.5	7	18	3.6
B3	WASS	7	19	20	8	17	71	14.2
B4	WASS	13	20	18	7	5	63	12.6
C4	WASS	2	6	2	1	4	15	3
A1	KAN	4.4	4.9	2	5.4	7.4	24.1	4.82
B3	KAN	4.9	14.2	12.7	7.8	3.4	43	8.6
B4	KAN	13.2	16.2	13.2	4.9	17	64.5	12.9
C4	KAN	3.9	7.8	2	0.5	2.9	17.1	3.42

Table 7. Measurements from the SEM and corresponding user readings

The ANOVA table to analyze the reproducibility of this technique is in Table 8.

ANOVA Table

Analysis of Variance

Source	Sum of Squares	Df	Mean Square	F-Ratio	P-Value
Between groups	33.0328	3	11.0109	0.27	0.8439
Within groups	3053.54	76	40.1782		
Total (Corr.)	3086.57	79			

Table 8. ANOVA table to validate reproducibility

From the above table it is seen that there is not significant difference between the means in each group at a 95% confidence interval. This suggests that the technique is proven to valid.

APPENDIX G. VARIATION IN ALIGNMENT AMONG THE WINDOWS

Level		Count	Mean	Error	Limit	Limit
GRAND MEAN		240	4.45729			
Thickness						
2		120	6.29292	0.363429	5.57648	7.00935
3		120	2.62167	0.363429	1.90523	3.3381
Size						
0.5		120	3.02875	0.363429	2.31231	3.74519
1		120	5.88583	0.363429	5.1694	6.60227
Window						
1		48	4.08333	0.574631	2.95055	5.21612
2		48	5.85625	0.574631	4.72346	6.98904
3		48	4.33229	0.574631	3.1995	5.46508
4		48	2.57708	0.574631	1.4443	3.70987
5		48	5.4375	0.574631	4.30471	6.57029
User						
Joe		80	4.30375	0.445107	3.4263	5.1812
Kan		80	4.36188	0.445107	3.48442	5.23933
Wass		80	4.70625	0.445107	3.8288	5.5837
Thickness by Size						
2	0.5	60	3.7325	0.513966	2.7193	4.7457
2	1	60	8.85333	0.513966	7.84014	9.86653
3	0.5	60	2.325	0.513966	1.3118	3.3382
3	1	60	2.91833	0.513966	1.90514	3.93153
Thickness by Window						
2	1	24	5.69167	0.812651	4.08966	7.29367
2	2	24	8.26667	0.812651	6.66466	9.86867
2	3	24	6.37708	0.812651	4.77508	7.97909
2	4	24	3.525	0.812651	1.923	5.127
2	5	24	7.60417	0.812651	6.00216	9.20617
3	1	24	2.475	0.812651	0.872997	4.077
3	2	24	3.44583	0.812651	1.84383	5.04784
3	3	24	2.2875	0.812651	0.685497	3.8895
3	4	24	1.62917	0.812651	0.0271638	3.23117
3	5	24	3.27083	0.812651	1.66883	4.87284
Thickness by User						
2	Joe	40	6.0175	0.629477	4.77659	7.25841
2	Kan	40	6.23625	0.629477	4.99534	7.47716
2	Wass	40	6.625	0.629477	5.38409	7.86591
3	Joe	40	2.59	0.629477	1.34909	3.83091
3	Kan	40	2.4875	0.629477	1.24659	3.72841
3	Wass	40	2.7875	0.629477	1.54659	4.02841

Size by Window						
0.5	1	24	3.3125	0.812651	1.7105	4.9145
0.5	2	24	3.6875	0.812651	2.0855	5.2895
0.5	3	24	2.18958	0.812651	0.58758	3.79159
0.5	4	24	2.08333	0.812651	0.48133	3.68534
0.5	5	24	3.87083	0.812651	2.26883	5.47284
1	1	24	4.85417	0.812651	3.25216	6.45617
1	2	24	8.025	0.812651	6.423	9.627
1	3	24	6.475	0.812651	4.873	8.077
1	4	24	3.07083	0.812651	1.46883	4.67284
1	5	24	7.00417	0.812651	5.40216	8.60617
Size by User						
0.5	Joe	40	2.99	0.629477	1.74909	4.23091
0.5	Kan	40	2.68375	0.629477	1.44284	3.92466
0.5	Wass	40	3.4125	0.629477	2.17159	4.65341
1	Joe	40	5.6175	0.629477	4.37659	6.85841
1	Kan	40	6.04	0.629477	4.79909	7.28091
1	Wass	40	6.0	0.629477	4.75909	7.24091
Window by User						
1	Joe	16	3.5875	0.995291	1.62546	5.54954
1	Kan	16	4.475	0.995291	2.51296	6.43704
1	Wass	16	4.1875	0.995291	2.22546	6.14954
2	Joe	16	5.0875	0.995291	3.12546	7.04954
2	Kan	16	5.95	0.995291	3.98796	7.91204
2	Wass	16	6.53125	0.995291	4.56921	8.49329
3	Joe	16	4.99375	0.995291	3.03171	6.95579
3	Kan	16	3.59687	0.995291	1.63483	5.55892
3	Wass	16	4.40625	0.995291	2.44421	6.36829
4	Joe	16	2.60625	0.995291	0.644205	4.56829
4	Kan	16	2.15625	0.995291	0.194205	4.11829
4	Wass	16	2.96875	0.995291	1.00671	4.93079
5	Joe	16	5.24375	0.995291	3.28171	7.20579
5	Kan	16	5.63125	0.995291	3.66921	7.59329
5	Wass	16	5.4375	0.995291	3.47546	7.39954

Table 9. Table with means from different combinations